Gas Phase Reactions between SiH_4 and B_2H_6: A Theoretical Study

Shao-Wen Hu,* Yi Wang, and Xiang-Yun Wang

Department of Applied Chemistry, College of Chemistry and Molecular Engineering, Peking University, Beijing, China 100871

Received: October 1, 2002; In Final Form: November 2, 2002

Gas-phase reactions of silane (SiH_4) and diborane (B_2H_6) are investigated using ab initio calculations at the MP2/6-311++g** level. Initially SiH_4 and B_2H_6 are only weakly attracted to each other. Under thermal activation, the two molecules can overcome an energy barrier of 33.87 kcal/mol to associate into a complex $SiH_4-BH_3-BH_3$ with a hydrogen-bridged Si−H−B bond. Upon bonding, one of the two hydrogen-bridged bonds B−H−B in B_2H_6 is broken and the other becomes polarized. Started from the $SiH_4-BH_3-BH_3$ complex, three comparable fragmentation pathways involving BH_3 and H_2 elimination produce several silaboranes with various silicon−boron−hydrogen ratios. A much higher barrier exists between the initial loosely bonded $SiH_4-B_2H_6$ system and a direct H_2 elimination product $SiH_3-B_2H_5$ with C_s symmetry. The bonding nature in the species are further elucidated through topological analysis of electron density using the AIM theory. These intermediate silaboranes are possible precursors for chemical vapor deposition in fabricating boron doped silicon films. Their composition and polarity may determine their tendency of surface adsorption and the properties of the relevant solid. The proposed mechanisms can help to understand and control the initial gas-phase reactions in practice. Calculated IR spectra, dipole moment, and rotational constants of the species are provided to facilitate experimental investigations.

I. Introduction

Silicon and boron hydrides SiH_4 and B_2H_6 are important source gases used in chemical vapor deposition (CVD) fabricating boron doped silicon thin films.[1−4] In the first stage of the process, energy is required to induce chemical reactions in the vapor. Evidences[5−7] show that smaller fragments such as radicals SiH_3 and molecules SiH_2 are produced as precursors for solid growth. It is also reported[8−10] that some clusters may exist and influence the quality of the solid. Clearly, the species formed from the gas phase is highly dependent on the experimental condition. As the information about the relationship between conditions and solid properties accumulates,[11−21] some theoretical mechanisms involving the gas phase and surface are also proposed.[22−27] In particular, on the observation that B_2H_6 can raise the silicon deposition rate to a certain extent in some experiments,[28,29] various boron−silicon hydrides are investigated theoretically.[30−32] It is not clear, however, what kinds of initial chemical reaction are actually induced between the two source-gas molecules SiH_4 and B_2H_6, and no detailed pathways have been traced to the small precursors formed from the original mixtures. In previous works,[33,34] we have demonstrated the existence of a hydrogen-bridged SiH_4-BH_3 complex. It is interesting to find out how the SiH_4-BH_3 complex is formed in the mixture of SiH_4 and B_2H_6. Two pathways are possible:

$$\text{(A) } B_2H_6 \rightarrow 2BH_3 \quad SiH_4 + BH_3 \rightarrow SiH_4-BH_3$$

$$\text{(B) } SiH_4 + B_2H_6 \rightarrow SiH_4-B_2H_6 \rightarrow SiH_4-BH_3 + BH_3$$

The key step toward a correct answer is to find out whether the intermediate or transition state of $SiH_4-B_2H_6$ exists or not. Because of the probable endothermic nature of the initial reaction, it would be difficult to detect or observe such transient intermediates. Therefore, we think that a theoretical investigation focused on the gas-phase reaction between SiH_4 and B_2H_6 neutral molecules would be very helpful and indispensable.

II. Calculation Method

All of the geometry structures were fully optimized at the MP2/6-31+G* level. Transition states were located using synchronous transit-guided quasi-Newton (STQN) methods[35] in combination with stepwise partial optimization along each pathway with one geometry parameter fixed as constant. Frequency calculations were performed following each optimization to obtain the zero-point energy (ZPE) and IR spectra data and to characterize all of the stationary points located on the potential energy surface. Single-point calculations at the MP2/6-311++g** level determine the electronic energies. The theoretical levels were shown to be suitable for the systems containing silicon and boron.[34] The Guassian 98 program package[36] was employed for these calculations.

Wave functions calculated at the MP2/6-31+G* level were used for the topological analyses of the electron densities. The AIM2000 program[37] derived from Bader's "atoms in molecules" (AIM) theory[38] was employed for calculating the bond critical points (BCP) and visualizing the bond paths.

III. Results and Discussions

As a Lewis acid, B_2H_6 can react with electron donors such as NH_3. Studies have shown that a slightly (∼5 kcal/mol) more stable complex $NH_3-(BH_3)_2$ forms over a barrier about 13 kcal/mol.[39] The $NH_3-(BH_3)_2$ complex is then subject to further BH_3 or H_2 elimination processes if sufficient energy is provided. SiH_4 can be regarded as a weak Lewis base albeit it donates a partially

* To whom correspondence should be addressed. E-mail: sw-hu@163.com.

10.1021/jp027113k CCC: $25.00
Published on Web 02/13/2003

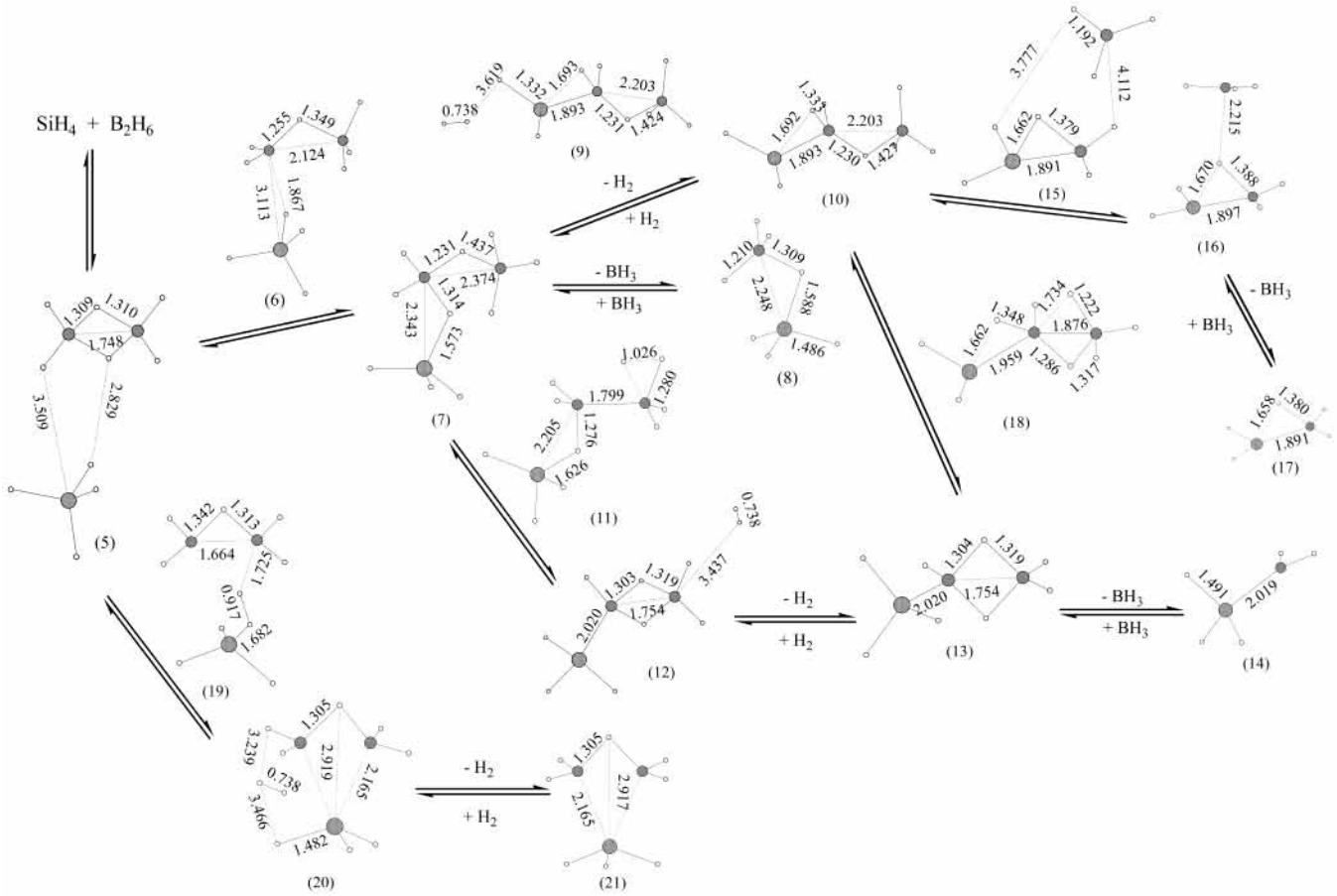

Figure 1. Optimized (MP2/6-31+G*) geometry structures of the intermediates (bond lengths in Å) in the reactions of SiH_4 and B_2H_6. The species above the double arrows are transition states.

TABLE 1: Electronic Energies, Dipole Moments, and Rotational Constants of the Species

no.	species	symm	E_e[a]/ a.u.	E_e[b]/ a.u.	ZPE[a] kcal/mol	dipole[a]/ Debye	dipole[b] Debye	rotational constants[a] [a]GHZ	GHZ	GHZ
1	H_2	$D_{\infty h}(0)$	−1.14414	−1.16030	6.48	0.000	0.000	0.000	1842	1842
2	BH_3	$D_{3h}(0)$	−26.46635	−26.51198	17.00	0.000	0.000	235.5	235.5	117.8
3	B_2H_6	$D_{2h}(0)$	−52.99703	−53.09251	40.90	0.000	0.000	80.66	18.52	17.00
4	SiH_4	$T_d(0)$	−291.31424	−291.49669	20.34	0.000	0.000	85.71	85.71	85.71
5	$SiH_4-B_2H_6$	$C_1(0)$	−344.31251	−344.59078	61.76	0.052	0.056	15.48	1.739	1.625
6	$SiH_4-B_2H_6$(t)	$C_1(1)$	−344.25308	−344.53392	59.95	2.670	2.657	12.76	2.687	2.371
7	$SiH_4-BH_3-BH_3$	$C_1(0)$	−344.26692	−344.55100	62.78	4.272	4.186	12.90	3.831	3.229
8	SiH_4-BH_3	$C_s(0)$	−317.78878	−318.02408	41.73	2.317	2.225	49.79	8.502	8.438
9	$H_2-SiH_2-B_2H_6$(t)	$C_1(1)$	−344.23402	−344.51339	56.85	4.520	4.515	14.04	2.881	2.556
10	$SiH_2-B_2H_6$	$C_1(0)$	−343.08962	−343.35270	49.93	4.484	4.483	23.97	3.643	3.337
11	$SiH_3-B_2H_5-H_2$(t)	$C_1(1)$	−344.23895	−344.52866	61.05	2.172	2.092	20.38	3.463	3.238
12	$SiH_3-B_2H_5-H_2$	$C_1(0)$	−344.30024	−344.57766	58.46	0.591	0.541	12.93	3.040	2.795
13	$SiH_3-B_2H_5$	$C_1(0)$	−343.15582	−343.41692	51.62	0.588	0.551	26.00	3.932	3.654
14	SiH_3-BH_2	$C_s(0)$	−316.62253	−316.83336	28.33	0.446	0.419	63.68	10.67	5.515
15	SiH2−BH3−BH3(t)	C1(1)	−343.08206	−343.34114	46.48	1.935	1.971	11.407	1.885	1.657
16	$SiH_2-BH_3-BH_3$	$C_1(0)$	−343.08377	−343.34396	47.46	2.172	2.235	11.45	3.681	3.018
17	SiH_2-BH_3	$C_s(0)$	−316.61497	−316.82834	29.26	1.906	1.945	75.50	12.28	11.29
18	$SiH_3-B_2H_5$(t)	$C_1(1)$	−343.08676	−343.35084	49.86	2.842	2.845	29.20	3.748	3.499
19	$B_2H_5-SiH_3-H_2$(t)	$C_1(2)$	−344.16423	−344.45925	59.62	3.184	3.084	14.04	4.309	3.732
20	$B_2H_5-SiH_3-H_2$	$C_1(1)$	−344.29940	−344.57614	58.34	0.676	0.701	7.552	5.543	4.880
21	$B_2H_5-SiH_3$	$C_s(0)$	−343.15497	−343.41530	51.60	0.692	0.712	14.47	7.120	10.21

[a] MP2/6-31+G* calculations. [b] MP2/6-311++G** calculations.

negative charged hydrogen instead of a lone electron pair. Based on our calculation, SiH_4 can associates with B_2H_6 and undergoes decomposition in several ways. Figure 1 shows the optimized geometry structures of the species involved in the first stage of the reactions. The corresponding energies, dipole moments, and rotational constants are listed in Table 1. Some characteristic IR data for the species are listed in Tables 3 and 4. Figure 2 shows molecular graphs of the species calculated using the AIM method. The proposed mechanisms and relative energies are presented in Figure 3 and Table 2.

A. $SiH_4-B_2H_6$ (5), the Initial Molecular Association of SiH_4 and B_2H_6. The position and orientation of SiH_4 relative to B_2H_6 are varied as initial structures for geometry optimization with or without symmetry constrains. The results indicate that

TABLE 2: Relative Energies of the Intermediate Species of the $SiH_4 + B_2H_6$ System

species	D_e[a]	D_e[b]	D_{e0}[c]
5	0.00	0.00	0.00
3 + **4**	0.78	0.99	0.47
2(**2**) + **4**	41.14	44.01	36.59
6	37.29	35.68	33.87
7	28.61	24.96	25.98
8+ **2**	36.00	34.33	31.31
9	49.25	48.56	43.66
10+ **1**	49.42	48.80	43.45
11	46.16	38.98	38.26
12	7.70	8.23	4.92
13+ **1**	7.87	8.50	4.85
14 + **2** + **1**	49.88	53.42	43.48
15 + **1**	54.16	56.06	47.26
16 + **1**	53.08	54.29	46.47
17 + **2** + **1**	54.62	56.58	47.56
18 + **1**	51.21	49.97	44.55
19	93.05	82.53	80.39
20	8.23	9.19	5.77
21 + **1**	8.41	9.53	5.85

[a] Relative electronic energies D_e (kcal/mol) calculated at the MP2/6-31+G*//MP2/6-31+G* level. See Table 1 for the species and Figure 1 for the structures. [b] Relative electronic energies D_e (kcal/mol) calculated at the MP2/6-311++G**//MP2/6-31+G* level. [c] Relative electronic energies D_{e0} (kcal/mol) calculated at the MP2/6-311++G**//MP2/6-31+G*+ ZPEC level.

the global minimum corresponds to a loosely bonded association $SiH_4-B_2H_6$ (**5**) with bonding energy less than 1 kcal/mol. The geometry parameters for each monomer in **5** are essentially same as isolated SiH_4 and B_2H_6. The bonding connections are drawn referring to its molecular graph calculated using AIM theory. It can be seen that two bond critical points are found between SiH_4 and B_2H_6. One mediates a terminal hydrogen of B_2H_6 and silicon of SiH_4, and the other mediates a bridged hydrogen of B_2H_6 and a hydrogen of SiH_4. The interactions, though very weak, show the probable specific sites of reactivity. The splitting of Si−H stretching vibrational frequency can be used as IR spectra evidence of the formation of **5**.

B. $SiH_4-BH_3-BH_3$ (7), the Intermediate Complex. When energy is provided, collision between SiH_4 and B_2H_6 could induced stronger interaction. As the two monomers in **5** approach closer, an intermediate complex $SiH_4-BH_3-BH_3$ (**7**) forms. Between **5** and **7**, a transition state structure $SiH_4-B_2H_6$-(t) (**6**) is located. The structure varies from **5** through **6** to **7**. A Si−H−B bond is gradually formed, whereas a B−H−B bond is gradually broken. The total process is endothermic. The energy of **7** is 25.98 kcal/mol higher relative to that of **5** calculated at the MP2/6-311++G**//MP2/6-31+G* + ZPE level. The activation barrier (energy of **6** relative to that of **5**) of the reaction is 33.87 kcal/mol. Compared with 36.12 kcal/mol, the dissociation energy of B_2H_6 to BH_3, the formation of **7** is slightly favored in energy. The significant increase in dipole moment from **5** to **6** to **7** indicates that the electron density is redistributed upon bonding. The highly polarized feature of **7** implies it is more likely to move in electrical field and could

TABLE 3: Selected (around B−H−B) Vibrational Frequencies of the Species[a]

		symm	B−H−B	B−H				
2	BH_3	$D_{3h}(0)$		2782(138)				
3	B_2H_6	$D_{2h}(0)$	1808(523)	2106(11)	2679(156)	2789(193)		
5	$SiH_4-B_2H_6$	$C_1(0)$	1807(491)	2108(10)	2678(147)	2774(2)	2788(193)	
6	$SiH_4-B_2H_6$(t)	$C_1(1)$	1771(100)	2308(245)	2581(12)	2675(1027)	2692(53)	2723(73)	2842(74)
7	$SiH_4-BH_3-BH_3$	$C_1(0)$	1548(68)	2402(411)	2575(22)	2625(55)	2664(153)	2693(115)	2734(70)
8	SiH_4-BH_3	$C_s(0)$	2561(19)	2649(104)	2720(105)				
9	$H_2-SiH_2-B_2H_6$(t)	$C_1(1)$	1524(220)	2417(244)	2581(19)	2680(131)	2686(98)	2777(53)	
10	$SiH_2-B_2H_6$	$C_1(0)$	1521(221)	2419(244)	2581(18)	2681(132)	2686(98)	2777(53)	
11	$SiH_4-B_2H_4-H_2$(t)	$C_1(1)$	2286(216)	2649(100)	2654(30)	2738(101)			
12	$SiH_4-B_2H_4-H_2$	$C_1(0)$	1775(599)	2681(111)	2702(48)	2780(96)			
13	$SiH_4-B_2H_4$	$C_1(0)$	1775(599)	2681(111)	2702(48)	2780(97)			
18	$SiH_3-B_2H_5$(t)	$C_1(1)$	1961(268)	2122(24)	2506(50)	2644(140)	2728(90)	2754(58)	
19	$B_2H_5-SiH_3-H_2$(t)	$C_1(2)$	1709(189)	2052(851)	2590(160)	2616(22)	2662(35)	2686(194)	
20	$B_2H_5-SiH_3-H_2$	$C_1(0)$	1883(150)	2161(32)	2636(104)	2650(9)	2737(13)	2751(144)	
21	$B_2H_5-SiH_3$	$C_s(0)$	1883(148)	2161(32)	2635(104)	2650(9)	2736(12)	2751(139)	

[a] Frequencies (not scaled) in cm^{-1}; intensities (in parentheses) in km/mol.

TABLE 4: Selected (around Si−H−B) Vibrational Frequencies of the Species[a]

		symm	Si−H−B		Si−H			
4	SiH_4	$T_d(0)$			2340(160)			
5	$SiH_4-B_2H_6$	$C_1(0)$			2322(31)	2331(143)	2337(156)	2340(138)
6	$SiH_4-B_2H_6$(t)	$C_1(1)$		2184(704)	2339(47)	2355(134)	2368(96)	
7	$SiH_4-BH_3-BH_3$	$C_1(0)$	1756(20)	2167(335)	2354(40)	2385(22)	2424(87)	
8	SiH_4-BH_3	$C_s(0)$	1801(23)	2054(334)	2308(114)	2371(55)	2395(98)	
9	$H_2-SiH_2-B_2H_6$(t)	$C_1(1)$	1325(257)	1919(78)	2336(86)	2360(82)	2791(33)	
10	$SiH_2-B_2H_6$	$C_1(0)$	1326(258)	1917(79)	2336(89)	2360(82)	2792(33)	
11	$SiH_4-B_2H_4-H_2$(t)	$C_1(1)$	1651(72)	2188(214)	2307(78)	2361(63)	2386(91)	2546(54)
12	$SiH_4-B_2H_4-H_2$	$C_1(0)$		2292(74)	2299(154)	2299(148)		
13	$SiH_4-B_2H_4$	$C_1(0)$		2292(74)	2299(154)	2300(149)		
14	SiH_3-BH_2	$C_s(0)$		2275(95)	2303(108)	2307(150)	2667(90)	2752(104)
15	SiH2−BH3−BH3(t)	$C1(1)$	1356(320)	1811(120)	2321(86)	2339(137)	2661(69)	2764(83)
16	$SiH_2-BH_3-BH_3$	$C_1(0)$	1331(259)	1753(313)	2327(83)	2346(109)	2670(52)	2776(49)
17	SiH_2-BH_3	$C_s(0)$	1356(329)	1812(126)	2322(93)	2340(133)	2665(69)	2769(75)
18	$SiH_3-B_2H_5$(t)	$C_1(1)$	1499(240)	1824(114)	2307 7(88)	2332(113)		
19	$B_2H_5-SiH_3-H_2$(t)	$C_1(2)$	1327(89)	1649(13)	2149(1190)	2327(43)	2358(79)	2378(66)
20	$B_2H_5-SiH_3-H_2$	$C_1(0)$			2320(52)	2331(91)	2363(94)	
21	$B_2H_5-SiH_3$	$C_s(0)$			2320(52)	2331(91)	2363(93)	

[a] Frequencies (not scaled) in cm^{-1}; intensities (in parentheses) in km/mol.

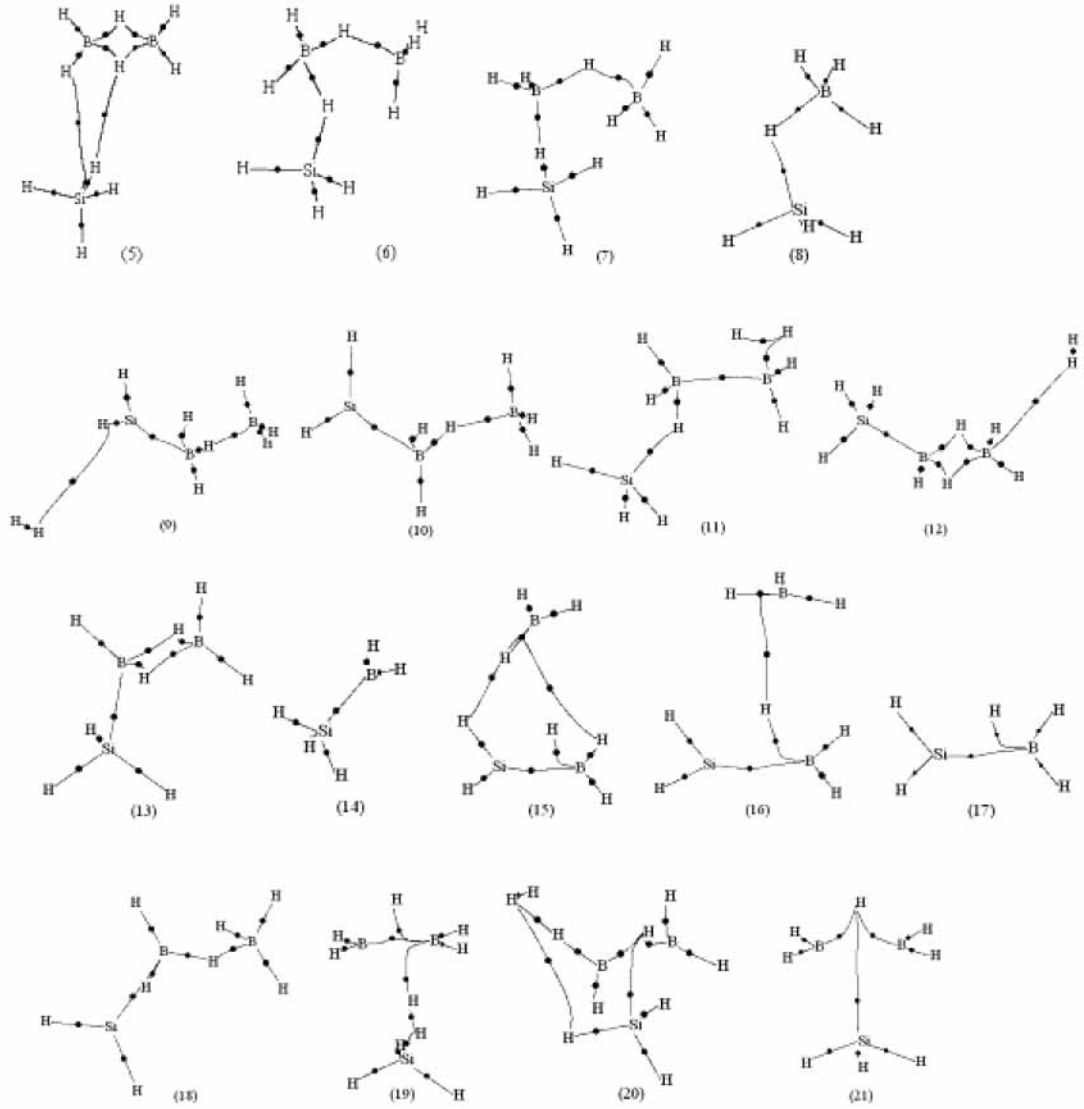

Figure 2. AIM (MP2/6-31+G*) calculated molecular graphs with bond paths and BCP of the species.

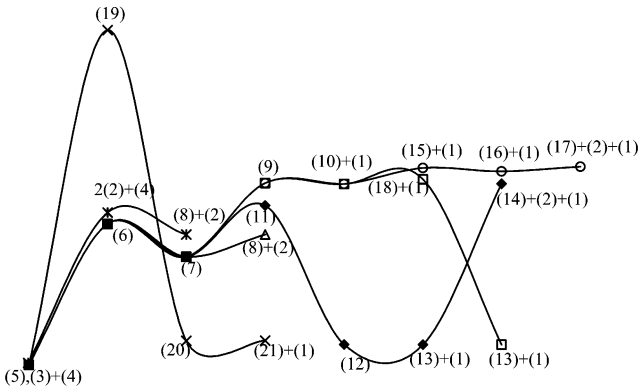

Figure 3. Reaction pathways of SiH_4 and B_2H_6, the height of each curve represents relative energies in kcal/mol based on calculations at the MP2/6-311++G**//MP2/6-31+G*+ZPE level. See Tables 1 and 2 for relevant species and energies.

be stabilized under plasma enhanced CVD conditions. The IR spectra characterizing the bridged Si−H−B stretching mode can be used as signals of the existence of **6** and **7**.

C. SiH_4-BH_3 (8), the BH_3 Elimination Product of 7. The geometry and molecular graph of $SiH_4-BH_3-BH_3$ (**7**) show that one of the original B−H−B bonds in B_2H_6 is clearly broken. The hydrogen atom in the remaining B−H−B bond moves closer to the boron connected with SiH_4, leaving a BH_3 monomer subjected to elimination. About 5 kcal/mol energy is required to dissociate **7** into SiH_4-BH_3 (**8**) and BH_3 (**2**). No transition states are located between **7** and **8** + **2**. The product **8** can also form through direct association of SiH_4 and BH_3. From Figure 3, we can see that the two pathways toward **8** are energetically comparable. As we have mentioned in previous work,[33,34] **8** is an electron donor-acceptor complex in which SiH_4 acts as electron donor. The electron-transfer effect results in the polarity of **7** and **8**. Further decomposition of **8** leading to smaller silaborane requires much more energy according to our calculation (not shown). Complexes **7** and **8** are, therefore, both probable precursors for solid deposition. Their polarity may promote the process in electrical fields. Compared with **7**, **8** is more compact and less polar. The back-donation from boron hydrogen to SiH_4, which is stronger for **8**, may account for the effects.

D. $SiH_2-B_2H_6$ (10) and $SiH_3-B_2H_5$ (13), the H_2 Elimination Products of 7. Starting from **7**, two H_2 elimination processes can occur besides the BH_3 elimination. First, the remaining bridged hydrogen and one of the terminal hydrogen atoms can connect to form a transition state structure $SiH_3-B_2H_5-H_2$(t) (**11**), which is about 12 kcal/mol higher in energy

than **7**. The H_2 eliminated product $SiH_3-B_2H_5-H_2$ (**12**) is a molecular association of $SiH_3-B_2H_5$ (**13**) and H_2. Therefore, the entire pathway from SiH_4 and B_2H_6 to a compound containing a Si−B bond is **5** → **6** → **7** → **11** → **12** → **13**. We can regard **13** as a derivative of B_2H_6 with one of the terminal hydrogen atoms replaced by a SiH_3. In an analogue way, **13** may be attacked by another SiH_4 and forms a SiH_3 derivative of **7**, or, directly dissociates into SiH_3-BH_2 (**14**) and BH_3. Alternatively, the H_2 to be eliminated may originate from a hydrogen atom of Si−H and the bridged H of Si−H−B bond. The transition state located is $H_2-SiH_2-B_2H_6$ (t) (**9**). It can be seen that **9** is just a loosely connection of $SiH_2-B_2H_6$ (**10**) and H_2. Compound **10** is energetically higher and more polar than its isomer **13**. Either **10** or **13** is probable precursor for deposition. The barrier for isomerization from **10** to **13**, determined by the relative energy of transition state structure $SiH_3-B_2H_5$ (t) (**18**), is small. Thus, the probability of **10** being a precursor may highly depend on the polarity of the environment.

E. SiH_2-BH_3 (17) and SiH_3-BH_2 (14), BH_3 Elimination Product of (10) and (13). It can be seen in Figure 3 that compound **10** is a quite unstable intermediate. Besides isomerization into **13**, it can undergo further fragmentation to produce SiH_2-BH_3 (**17**). A BH_3 half eliminated cluster $SiH_2-BH_3-BH_3$ (**16**) mediates the process and a transition state $SiH_2-BH_3-BH_3$(t) (**15**) is located between **10** and **16**. Dissociation of **13** into SiH_3-BH_2 (**14**) and BH_3 requires more energy and appear to be straightforward because no transition states are located. Compound **14** can be regarded as a derivative of BH_3. Boron is three coordinated in **14**. Compound **17** is a less stable and more polar isomer of **14**. Unlike **14**, both silicon and boron in **17** are nearly four coordinated through a partially formed Si−H−B bridged bond. This structural character and their different polarity may determine their performance as precursors for solid deposition. The vibrational frequencies of **17** reflect the presence of the Si−H−B bond, which is clearly absent in **14**.

F. $SiH_3-B_2H_5$ (20), the Direct H_2 Elimination Product of (5). An interesting structure $B_2H_5-SiH_3$ (**21**) with C_s symmetry can be obtained by direct H_2 elimination from **5**. The transition state $B_2H_5-SiH_3-H_2$ (t) (**19**) represents a barrier much higher than the other mechanism pathways. $B_2H_5-SiH_3-H_2$ (**20**) is a loose association of **21** and H_2. The connectivity of **21** revealed by the AIM molecular graph shows that silicon is four coordinated and bonded with a bridged-hydrogen atom. That is, silicon, two boron atoms, and the bridged-hydrogen compose a four-center−four-electron bond. Despite the high activation energy, the formation of **21** is not very endothermic, in contrary to other dissociations. Therefore, **21** and **13** are two stable products probably formed during initial gas-phase reactions of SiH_4 and B_2H_6. Further investigation is necessary to character this compound.

IV. Concluding Remarks

The detailed theoretical investigation of gas-phase reactions between SiH_4 and B_2H_6 demonstrates several possible pathways connecting the reactants and the products. When sufficient energy is provided, the energetically favored intermediate is the associated complex $SiH_4-BH_3-BH_3$ (**7**). SiH_4-BH_3 (**8**) is the BH_3 eliminated product of **7**. Two possible H_2 elimination pathways lead **7** to $SiH_3-B_2H_5$ (**13**) and $SiH_2-B_2H_6$ (**10**), which in turn, can dissociate into smaller fragments SiH_3-BH_2 (**14**) and SiH_2-BH_3 (**17**), respectively. Another pathway through direct H_2 elimination from molecular association of SiH_4 and B_2H_6 has a much higher energetic barrier. The corresponding product $B_2H_5-SiH_3$ (**21**), however, is quite stable. These intermediate silaborane compounds, different in composition, polarity, and geometry structure, may play specific roles as precursors in CVD processing boron doped silicon films. Their characteristic IR spectra are provided for experimental identifications.

References and Notes

(1) Waltenburg, H. N.; Yates, J. T. *Chem. Rev.* **1995**, *95*, 1589.

(2) Wang, Y. J.; Shan, J.; Hamers, R. J. *J. Vac. Sci. Technol. B* **1996**, *14*, 1038.

(3) Sanganeria, M. K.; Violette, K. E.; Ozturk, M. C.; Harris, G.; Maher, D. M. *J. Electrochem. Soc.* **1995**, *142*, 285.

(4) Habuka, H.; Akiyama, S.; Otsuka, T.; Qu, W. F. *J. Cryst. Growth* **2000**, *209*, 807.

(5) Chattopadhyay, S.; Das, D.; Sharma, S. N.; Barua, A. K.; Banerjee, R.; Kshirsagar, S. T. *Jpn. J. Appl. Phys. 1* **1995**, *34*, 5743.

(6) Gourbilleau, F.; Achiq, A.; Voivenel, P.; Rizk, R. *Solid State Phenom.* **1999**, *67*, 137.

(7) Gong, B.; Brown, D. E.; Kang, J. H.; Jo, S. K.; Sun, Y. M.; Ekerdt, J. G. *Phys. Rev. B* **1999**, *59*, 15225.

(8) Hess, G.; Parkinson, P.; Gong, B.; Xu, Z.; Lim, D.; Downer, M.; John, S.; Banerjee, S.; Ekerdt, J. G.; Jo, S. K. *Appl. Phys. Lett.* **1997**, *71*, 2184.

(9) Meloni, G.; Gingerich, K. A. *J. Chem. Phys.* **2001**, *115*, 5470.

(10) Cowern, N. E. B.; Mannino, G.; Stolk, P. A.; Roozeboom, F.; Huizing, H. G. A.; van Berkum, J. G. M.; Cristiano, F.; Claverie, A.; Jaraiz, M. *Phys. Rev. Lett.* **1999**, *82*, 4460.

(11) Caputo, D.; de Cesare, G.; Nascetti, A.; Palma, F. *Thin Solid Films* **1999**, *348*, 79.

(12) Isomura, M.; Kinoshita, T.; Tsuda, S. *J. Non-Cryst. Solids* **1996**, *200*, 453.

(13) Pietruszko, S. M.; Pachocki, M.; Jang, J. *J. Non-Cryst. Solids* **1996**, *200*, 73.

(14) Nakamura, K.; Masuda, K.; Shigeta, Y. *Surf. Sci.* **2000**, *454*, 21.

(15) Fujita, K.; Ichikawa, M. *Surf. Sci.* **2000**, *468*, 85.

(16) Lin, S. Y. *Thin Solid Films* **1999**, *344*, 285.

(17) Voz, C.; Peiro, D.; Bertomeu, J.; Soler, D.; Fonrodona, M.; Andreu, J. *Mat. Sci. Eng. B−Solid* **2000**, *69*, 278.

(18) Niira, K.; Hakuma, H.; Komoda, M.; Fukui, K.; Shirasawa, K. *Sol. Energ. Mat. Sol. C* **2001**, *69*, 107.

(19) Pietruszko, S. M.; Jang, J. *Sol. Energ. Mat. Sol. C* **2002**, *71*, 459.

(20) Jadkar, S. R.; Sali, J. V.; Takwale, M. G.; Musale, D. V.; Kshirsagar, S. T. *Sol. Energ. Mat. Sol. C* **2000**, *64*, 333.

(21) Ferreira, I.; Fortunato, E.; Martins, R.; Vilarinho, P. *J. Appl. Phys.* **2002**, *91*, 1644.

(22) Habuka, H.; Otsuka, T.; Qu, W. F.; Shimada, M.; Okuyama, K. *J. Cryst. Growth* **2001**, *222*, 183.

(23) Lengyel, I.; Jensen, K. F. *Thin Solid Films* **2000**, *365*, 231.

(24) Jensen, K. F.; Rodgers, S. T.; Venkataramani, R. *Curr. Opin. Solid State Mater.* **1998**, *3*, 562.

(25) Wang, S. W.; Radny, M. W.; Smith, P. V. *Surf. Sci.* **1997**, *394*, 235.

(26) Simka, H.; Willis, B. G.; Lengyel, I.; Jensen, K. F. *Prog. Cryst. Growth Ch.* **1997**, *35*, 117.

(27) Wang, L. G.; Clancy, P.; Thompson, M. O.; Murthy, C. S. *J. Appl. Phys.* **2002**, *92*, 2412.

(28) Perrin, J.; Takeda, Y.; Hirano, N.; Takeuchi, Y.; Matsuda, A. *Surf. Sci.* **1989**, *114*, 210.

(29) Fresquet, G.; Azzaro, C.; Couderc, J. P. *J. Electrochem. Soc.* **1995**, *142*, 538.

(30) Ho, P.; Colvin, M. E.; Melius, C. F. *J. Phys. Chem. A* **1997**, *101*, 9470.

(31) Allendorf, M. D.; Melius, C. F. *Surf. Coat. Techol.* **1998**, *109*, 191.

(32) Allendorf, M. D.; Melius, C. F. *J. Phys. Chem. A* **2002**, *106*, 6370.

(33) Hu, S. W.; Kim, J.; Tarakeshwar, P.; Kim, K. S. *J. Phys. Chem. A* **2002**, *106*, 6817.

(34) Hu, S. W.; Wang, X. Y. *J. Phys. Chem. A* **2002**, *106*, 9558.

(35) Peng, C. Y.; Ayala, P. Y.; Schlegel, H. B.; Frisch, M. J. *J. Comput. Chem.* **1996**, *17*, 49.

(36) Frisch, M. J.; Trucks, G. W.; Schlegel, H. B.; Scuseria, G. E.; Robb, M. A.; Cheeseman, J. R.; Zakrzewski, V. G.; Montgomery, J. A., Jr.; Stratmann, R. E.; Burant, J. C.; Dapprich, S.; Millam, J. M.; Daniels, A. D.; Kudin, K. N.; Strain, M. C.; Farkas, O.; Tomasi, J.; Barone, V.; Cossi, M.; Cammi, R.; Mennucci, B.; Pomelli, C.; Adamo, C.; Clifford, S.; Ochterski, J.; Petersson, G. A.; Ayala, P. Y.; Cui, Q.; Morokuma, K.; Malick, D. K.; Rabuck, A. D.; Raghavachari, K.; Foresman, J. B.; Cioslowski, J.; Ortiz, J. V.; Stefanov, B. B.; Liu, G.; Liashenko, A.; Piskorz, P.; Komaromi,

I.; Gomperts, R.; Martin, R. L.; Fox, D. J.; Keith, T.; Al-Laham, M. A.; Peng, C. Y.; Nanayakkara, A.; Gonzalez, C.; Challacombe, M.; Gill, P. M. W.; Johnson, B. G.; Chen, W.; Wong, M. W.; Andres, J. L.; Head-Gordon, M.; Replogle, E. S.; Pople, J. A. *Gaussian 98*, revision A.7; Gaussian, Inc.: Pittsburgh, PA, 1998.

(37) Biegler-Konig, F.; Schonbohm, J.; Bayles, D. *J. Comput. Chem.* **2001**, *22*, 545.

(38) Bader, R. F. W. *Atoms in Molecules: A Quantum Theory*; Oxford University Press: Oxford, U.K., 1990.

(39) Mckee, M. L. *J. Phys. Chem.* **1992**, *92*, 5380.